Desalination and Water Treatment
www.deswater.com

doi:10.5004/dwt.2017.20791

79 (2017) 356–367
June

Adsorption of Reactive Red 2 using activated carbon prepared from walnut shell: batch and fixed bed studies

Ali Almasi, Zeinab Rostamkhani, Seyyed Alireza Mousavi*

Department of Environmental Health engineering and Research Center for Environmental Determinants of Health (RCEDH), Kermanshah University of Medical Sciences, Kermanshah, Iran, Tel. 9809181317314, email: alialmasi@yahoo.com (A. Almasi), z.rostamkhani90@gmail.com (Z. Rostamkhani), Tel. +9809188336569, email: seyyedarm@yahoo.com, sar.mousavi@kums.ac.ir (S.A. Mousavi)

Received 15 September 2016; Accepted 8 April 2017

ABSTRACT

The preparation of activated carbon from walnut shell with $ZnCl_2$ activation and its ability to remove Reactive Red 2 from aqueous solutions was studied through batch and column study. The adsorbent was characterized with BET, FTIR, and SEM. Batch-adsorption technique was conducted to investigate the effects of parameters namely; pH, absorbent dose, contact time, and initial dye concentration on the adsorption efficiency. In column study, the effects of initial dye concentration, bed height and flow rate on Reactive Red 2 (RR2) adsorption were studied. In batch system, the adsorption efficiency at a dose of 1.5 g/L and pH 2 was achieved by 65.55%. Data were fitted with Langmuir isotherm equilibrium. The maximum capacity based on Langmuir model was 81.3 mg/g. The results showed that by increasing the concentration of color on continuous input from 50 to 150 mg/L the adsorption capacity has increased from 42.18 to 53.72 mg/g, respectively. With the increase in height of column from 2 to 8 cm the adsorption capacity increased from 37.28 to 54.61 mg/g. Furthermore, with increases of flow rate from 5 to 15 ml/min the adsorption capacity decreased from 51.81 to36.67 mg/g.

Keywords: Adsorption; Agricultural wastes; Dye; Fixed bed

1. Introduction

Use of different chemical compounds in industrial processes, such as cosmetics, leather, paper and textile produces large volumes of colored effluents containing organic and inorganic pollutants that suitable treatment of them is environmental requirements. The amount of produced dye is estimated to be 1,000,000 tons per year [1,2]. The first known contaminants in wastewater are dyes, that small amounts of them in water (less than 1 ppm for some dyes) is highly visible and undesirable [3]. The COD of effluent increases because of high concentration of dyes in the influent of wastewater treatment plants, due to the complex structure that are stable and non-biodegradable. They also are toxic, carcinogenic, mutagen and can cause allergies and skin problems [4]. Furthermore, the dyes in industrial wastewater due to their toxicity on aquatic organisms, impaired performance of sewage treatment systems, and they are considered for aesthetic environment. Discharging of colored wastewater into receiving waters body, may leads to interference phenomena in ecology such as eutrophication due to the presence of nitrogen [5]. They can affect aquatic flora and fauna to a great extent [6]. The concentrations of these contaminants for discharging into natural resources should be reduced to a set of standards, because if they cannot be properly removed, have serious negative effects on human health and environment.

Dye removal can be divided to 3 methods namely; biological, chemical and physical [7]. Methods that are currently used for treating dyes have technical and economical limitations. The most of physicochemical methods have been used for dye removal from aqueous environments are expensive, and produce large quantities of sludge. In addition, some water-soluble dyes cannot be removed completely by aforementioned methods. Biological removal of

---

*Corresponding author.

1944-3994 / 1944-3986

dyes may be cheaper than physicochemical methods, but some of the resistant dyes are toxic for microorganisms [8]. Among them the absorption process due to many advantages such as simplicity of design, ease of operation and insensitivity to toxic substances is preferred over other methods.

Activated carbon (AC) due to high efficacy has been widely used for absorption. However, its use is limited because of high price [9]. In recent years, agricultural wastes such as rice bran, wheat, barley, rice stalks, wood waste and bagasse have been used for removal of toxic metals and some organic contaminants from aqueous solutions [10]. Walnut shell due to the high content of carbon and low ash is suitable for the activated carbon production [11].

Development of low-cost adsorbent for reducing the cost of adsorption process from agricultural waste could be a good alternative for commercial activated carbon [12]. Ministry of Agriculture in Iran reported that over 170,000 tons per year walnut produces, which this country has grade third in world. Therefore, walnut shell as cheap, local and available waste can be used for producing of activated carbon [13].

Walnut shell wastes have been used for producing of AC as adsorbent for the removal of methylene blue from aqueous solutions. Results of study by Yang and Qiu [11] showed the highest capacity was 315 mg/g for the optimum dosage of AC. Wang et al. [14] studied the removal of chromium (VI) from aqueous solution using walnut hull. The results showed the maximum removal of Cr (VI) was 97.3% at pH 1. In another study Cao et al. [15] investigated the potential of biosorbent, chem-modified walnut shell for removal of reactive brilliant red K-2BP.

Most previous studies on the adsorption of dye and other pollutants on prepared activated carbon by walnut shell (WSAC) have focused on batch kinetic and batch equilibrium investigations. However, in full scale the fixed-bed columns are often preferred, which design and optimization of fixed-bed columns are difficult without prior study in bench and pilot scale. In this regard, the efficiency of activated carbon prepared from walnut shell for the removal of Reactive Red 2 (RR2) has been investigated in both batch and continuous conditions using a laboratory scale fixed bed column. Furthermore, the main design parameters such as pH of solution, initial concentration of dye, absorbent dose, contact time, column bed height, and flow rate of fluid on RR2 adsorption have been investigated. The isotherms and kinetics models are used to describe the distribution of dye between solid phase and the solution and to correlate the adsorption kinetics data of RR2 onto prepared WSAC. The processes of removal of the selected dyes on WSAC are investigated by Thermodynamic studies. The breakthrough curve for the adsorption of RR2 was studied using Thomas model.

2. Materials and methods

2.1. Dye and sorbent

All reagents used in this work were analytical reagent grade. In all experiments, synthetic solution of reactive red 2 as mono azo dye was prepared from the commercial product with formula ($C_{19}H_{10}Cl_2N_6Na_2O_7S_2$; 98% , MW = 615) supplied by E. Merck (Fig. 1). Walnut shell was obtained from Kermanshah rural area in the western region of Iran. Walnut shell collected from fallen pieces under the trees or during industrial process, when corn of walnut has been separated for using its nut. The walnut wastes were collected in plastic bags and transported to the laboratory where further testing procedures were carried out.

2.2. Preparation of activated carbon from walnut shell

In order to eliminate waste such as debris and dust, Walnut well-cleaned and washed and dried at room temperature. Walnut shells were crushed using a regular type jaw crusher. Crushed shells were dried for 1 h in the oven at 105ºC. The activation agent $ZnCl_2$ (with 98% purity, Merck Germany) was used for the preparation of activated carbon during 24 h with the weight ratio of 1:1 for $ZnCl_2$ to walnut shell.

Then, to perform the activation, Walnut shells were heated in a furnace to a final temperature of 500ºC for 1 h. For all treatments, the nitrogen gas at flow rate of 150 ml/min was applied in the reactor to create a condition without oxygen. The samples, was then left to cool at present of N_2, and washed several times to remove residues of $ZnCl_2$. To remove residue the activated carbon was saturated into a solution of 1.0 m HCl, then washed with distilled water until the pH of the solution reached to 7, and dried in an oven at 105ºC. Finally, the prepared activated carbon crushed and sieved to achieve different size fractions with 0.5–1 mm in diameter.

2.3. Batch equilibrium studies

This empirical study carried out at a laboratory bench scale by using walnut shell activated carbon (WSAC) for removing RR2 from aqueous solution. The walnut shall as granular activated carbon was applied to remove RR2 by using batch and Fixed-Bed reactor. At the first stage of experimental work, a series of batch tests were employed to investigate the dye removal from synthetic wastewater. The adsorption process has been conducted at the different values of independent variables; pH (2–11), adsorption dosage (0.2, 0.4, 0.6, 0.8, 1, 1.2, 1.5 mg/L), contact time (5, 30, 60, 90, 120, 150 min), and initial concentration of dye (50, 100, and 150 mg/L), using a series of Pyrex glass with total vol-

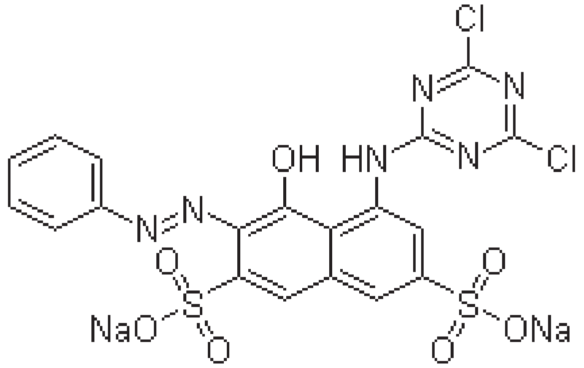

Fig. 1. The structural formula for RR 2.

ume of 250 mL and working volume of 100 mL, when other parameters were constant (e.g. ambient temperature (28 ± 1ºC), and mixing speed 100 rpm). The residual concentration was determined by measuring its absorbance in a UV-Visible spectrophotometer (JENWAY 6305, UK) at the maximum wavelength of 538 nm after centrifuge of sample at 3800 rpm for 5 min. The thermodynamic study carried out at different temperatures (20, 30, 40°C) to evaluate of temperature effect. The amount of adsorbed dye and percentage removal of RR2 were calculated by following equations

$$q_e = \frac{\left(C_\circ - C_e\right)V}{M} \tag{1}$$

$$R\% = \frac{C_0 - C_e}{C_0} \times 100 \tag{2}$$

where C_0 and C_e are the initial, final dye concentrations (mg/L), respectively; q_e is the amount of adsorbate per mass of the adsorbent (mg/g), V is the volume of solution (L); and M is the mass of adsorbent (g).

2.4. Column studies

The column studies have been conducted in a glass column made of Pyrex glass tube as fixed bed reactor with 1.2 cm inner diameter and 19.5 cm height. A layer of glass wool used as supporter at the bottom and top of activated carbon bed inside column based on desired height of carbon (2, 4, 8 cm). At first stage to remove dust on surface of applied WSAC, distillated water sparged on the bed by peristaltic pump for 15 min. Then the main part of present study, investigation of two main variables namely; dye concentrations (50, 100 and 150 mg/L), flow rate (5, 10 and 15 ml/min) have been carried out at pH 2. At the outlet of the column, effluent was collected at regular time intervals (one hour) and after centrifuge at 3800 rpm for 5 min, the concentration of RR2 was measured using a UV-visible spectrophotometer at 538 nm. All the experiments were carried out at room temperature (28 ± 1°C). The breakpoint and saturation condition was considered when the effluent concentration reached to 5% and 90% of influent concentration of dye, respectively. The absorbent behavior has been investigated by using Tomas Model, which is regular model to predict of failure curve in column bed of activated carbon. This model according to Eq. (3) can estimate the value of absorbed dye per unit mass of adsorbent in the column [16].

$$\ln\left(\frac{C_i}{C_e} - 1\right) = K_{Th} + \frac{q_0 M}{Q} - K_{Th} C_i t \tag{3}$$

where K_{Th} is the Thomas rate constant (ml/(min mg), q_o maximum adsorption (mg/g) and Q is the volumetric flow rate (mL/min), M is the total weight of the sorbent loaded in the column (g), C_i and C_e are dye concentrations (mg/L) in the influent and effluent, respectively.

2.5. Thermal regeneration of activated carbon

The regeneration study carried out by adding 300 mg of activated carbon into a 200 mL dye solution (100 mg/L), and the suspension was mechanically agitated (100 rpm) for 145 min at pH 2. The solution was then filtered, and the concentration of dye was calculated. The used activated carbon was loaded into the furnace, heated at 500°C for 60 min during sparging N_2 with 150 ml/min, and then allowed to cool down at room temperature at present of N_2. Subsequently, the adsorption experiment was carried out again to evaluate the regeneration efficiency of carbon, which was calculated according to the following equation [17]:

$$R = \frac{M_{rc}}{M_{vc}} \times 100 \tag{4}$$

where M_{rc} and M_{vc} are amounts adsorbed on regenerated and virgin carbon, respectively.

2.6. Characterization of activated carbon

The textural properties of WSAC were investigated by N_2 adsorption (at 77K) using Belsorp mini II, Japan (BEL Japan, Inc.). The surface area were estimated the Brunauer-Emmett-Teller (BET) method.

Scanning electron microscopy (SEM) was used to study surface morphology of both raw walnut shell and WSAC. The samples were sited under a JEOL JSM field-emission SEM. During operation, the accelerating voltage of the instrument was maintained at 15 kV and varying magnifications were used.

Fourier transform infrared spectroscopy (FTIR) of the adsorbent was obtained by using an FTIR spectrophotometer (Model: FTIR 2000, Shimadzu IR Prestige, Japan) to investigate the surface characteristics of absorbant.

3. Result and discussion

3.1. Surface area and pore size distribution

Fig. 2 shows the adsorption isotherm of nitrogen at 77 K. Nitrogen adsorption isotherm is type I, indicating that most of the openings are in the range of micro-porosity 2 nm. The results show that the produced WSAC has a surface area equal to 1110 m^2/g and the pore volume is equal to 0.453 cm^3/g.

Scanning electronic microscopy as primarily tool is generally used to investigate the morphological and surface characteristics of the adsorbent materials [18,19]. In this study, the surface structure of WSAC and raw walnut shell were analyzed and the structure examination can be observed from the SEM images (Fig. 3a,b). The SEM pictures of adsorbent show very distinguished irregular shape and dark spots that seem to have some degree of porosity. The high porosity is result of good activation performance. Therefore, it can play important role for preparing available surface for adsorption of RR2 onto WSAC.

At the present research, to determine the chemical structure and functional groups of the prepared activated carbon FTIR spectrum of WSAC, has been carried out according to Fig. 4. A broad band located around 3411 cm^{-1} is typically attributed to the hydroxyl groups or adsorbed water. The band around 1047 cm^{-1} is usually caused by the stretching vibration of C==O, while the band around 670 cm^{-1} is fingerprint zone. Dahri et al. (2014) indicates the presence of various functional groups at wavelengths 3373 cm^{-1} (O–H stretch), 2923 cm^{-1} (C–H stretch) [20]. The bands at1625 cm^{-1} probably indicate the bending vibration of H–O–H from absorbed water and the weak peak at 1453 cm^{-1} was ascribed to the stretching vibration of C=C in the benzene [21]. An intense band at around 1051 cm^{-1} can be attributed to C–O stretching vibrations in alcohols, phenols, ether or ether groups [15]. The region below 1000 cm^{-1} was the 'fingerprint zone' and the absorption could not clearly be assigned to any particular vibration because they corresponded to complex interacting vibration systems [22].

3.2. Effect of contact time

The results showed that with increasing contact time, removal rate at different concentrations of dye (50–150 mg/L) increased when the other variables were constant. Moreover, as shown in Fig. 5, adsorption efficiency slowly increased with an increase in contact time within the first minutes of process. Then, the rate of adsorption was found to be relatively slow and finally constant. This is because of a great number of adsorption sites at the beginning of process, the large difference between the concentration of dye in the absorbing solution and its value in the absorbent surface, that dye uptake is increased. Nevertheless, over time, the gentle slopes attract to itself that this is due to the development of a layer of dye onto the adsorbent. Also over time, occupy the place that left vacant of surface simply is not possible. Because the adsorption of molecules on the surface of other molecules in the solution phase is attractive, this can be case of repulsive onto absorbent surface [23,24]. For absorbent reaching for balance, time happens in the first 150 min of adsorption and not significant variation after that. This results has been confirmed by other researchers that the initial concentration strongly affects adsorption capacity [25,26]

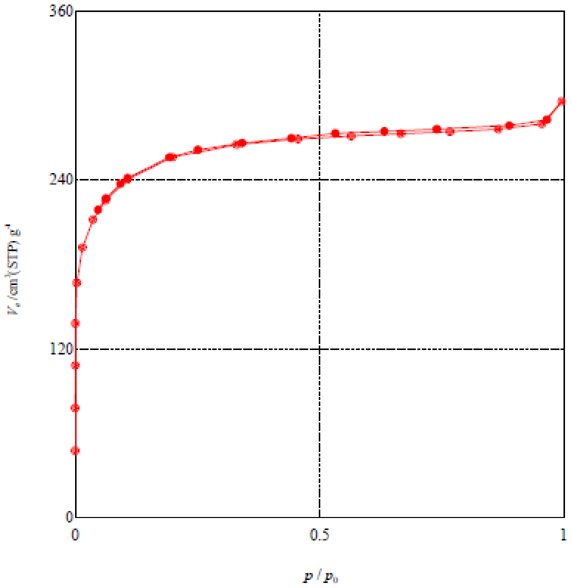

Fig. 2. Adsorption/desorption isotherm of nitrogen at 77 K.

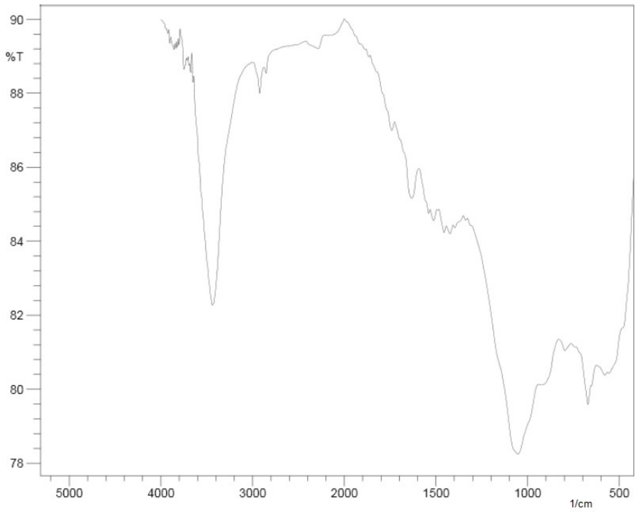

Fig. 4. FT-IR spectrum of the adsorbent WSAC.

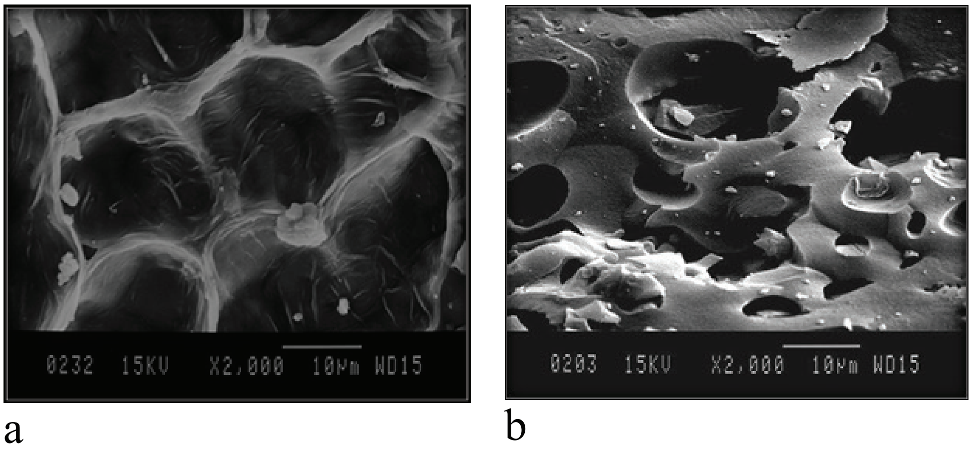

Fig. 3. Scanning electron microscope photographs of raw walnut shell (a) and prepared activated carbon (b) segment with same magnification factors.

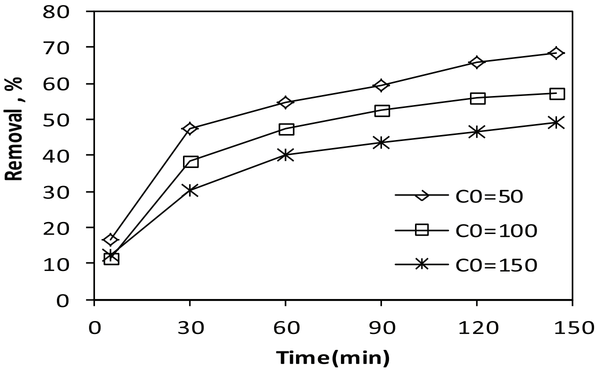

Fig. 5. Effect of contact time on adsorption of RR2 onto WAC at different initial concentrations of RR2 (Absorbent dosage = 1 g/l, pH = 2).

3.3. Effect of pH

The pH of the solution plays an important role in the whole process and absorptive capacity. The pH value not only has effect on surface charge, but also affects the degree of ionization and dissociation of solute, functional groups in the active sites of the adsorbent [27,28]. Therefore, pH as an important factor, which affecting the efficiency of the system was studied. For determining the optimum pH for adsorption, 10 pH values have been selected and the pH of solution was adjusted at the wanted value (2–11). Effect of pH on the efficiency removal of dye indicated that the percentage removal of RR2 increased with decreasing pH of the solution (Fig. 6). This is because at the low pH adsorbent surface is positively charged and the anionic dye RR2 is the category caused electrostatic attraction forces between the adsorbent and color to enhance the absorption capacity. The study has been done by Zeng on the adsorption of RR2 by using inorgano-organo pillared bentonite, the results showed that the maximum removal of dye achieved at acidic pH [29]. Manoochehri et al. (2010) studied the effect of pH on the removal of Reactive Yellow 15 and Reactive Black 5 from synthetic textile wastewater by using activated carbon walnut shell, the results showed that the maximum removal of dye at pH 2 occurred [30].

3.4. Effect of initial absorbent dose

The results of this investigation according to Fig. 7 showed that with increasing of adsorbent dose the dye removal increased, however, the adsorption capacity decreased. The maximum removal rate of 57.47% was observed when the dose of absorbent was 1.5 g/L. Increasing the amount of absorbent means increasing adsorbent surface, subsequently increases access to absorption sites for dye molecules, which can be cause of quick adsorption of dye. This reduces the available colors for maximum coverage, which leads to a reduction in the amount of adsorbed dye per unit weight of the absorbent [28]. The absorbent capacity is affected by changing absorbent dose as absorbent dose increased from 0.2 to 1.5 g/l the absorbent capacity decreased from 53.1 to 38.31 mg/g (Fig. 7). Dahri and coworkers achieved same result for investigation the effect

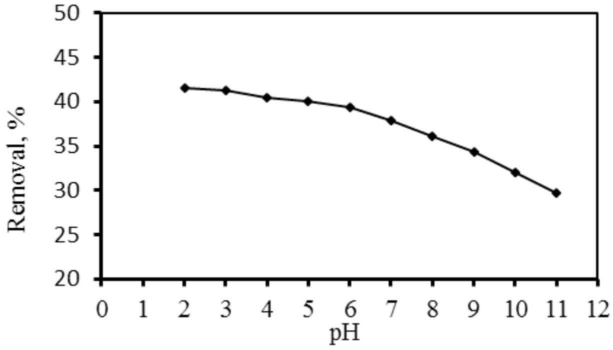

Fig. 6. Effect of pH on adsorption on adsorption of RR2 on WSAC. (Absorbent dosage = 1 g/l, dye concentration = 100 mg/l, contact time = 145 min).

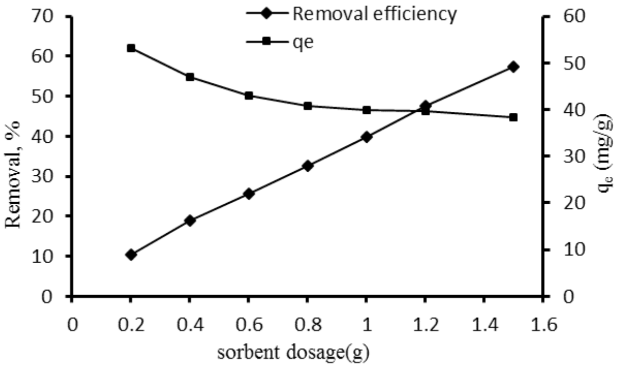

Fig. 7. Effect of adsorbent concentrations on the adsorption of RR2 onto WAC (dye concentrations = 100 mg/l, pH 2, contact time = 145 min).

of the initial absorbent concentration on the adsorption process [20].

3.5. Effect of initial concentration of dye

To investigate the effect of initial dye concentration on the removal rates, concentrations of 50, 100 and 150 mg/l of dye when other variables were constant was studied (Fig. 8). The highest removal efficiency equal to 68.55% was observed at the best value of variables. However, since the initial concentration was 150 mg/L the dye removal decreased to % 49.22. It can be pointed out that adsorbent has restricted specific adsorption sites and at the low concentrations of dye, greater adsorption sites are available on the adsorbent surface, resulting high rate of absorption. The effect of initial dye on the adsorption capacity showed that with increase of dye concentration from 50 to 150 mg/L the capacity of adsorption increased (Fig. 8), which the highest adsorption capacity was equal to 49.22 mg/l. The mass transfer increases with increasing initial dye concentration, which this phenomenon has overcome the force of resistance against adsorption, and creates a significant driving force for the transfer of pollutants from the liquid phase to the interface adsorbent-liquid, and it increases the effi-

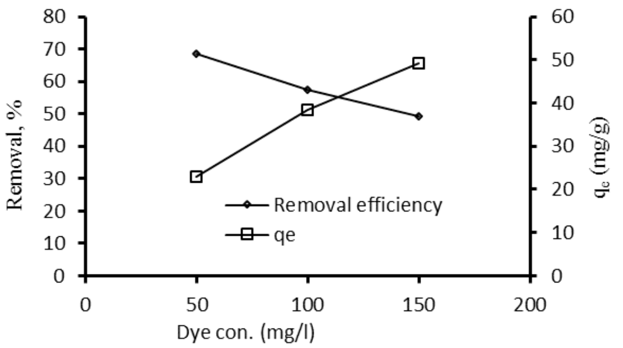

Fig. 8. Effect of initial dye concentrations on the adsorption of RR2 on WAC (Absorbent dosage = 1.5 g/l, pH = 2, contact time = 145 min).

ciency of absorption [31]. Same result have been reported by Auta and Hameed [32].

3.6. Effect of temperature

To investigate the effect of temperature, adsorption studies of Reactive Red 2 onto activated carbon prepared from walnut shell was accomplished at three different temperatures (20, 30, and 40°C). To better understand the influences of temperature on the adsorption of RR2 on WSAC, three thermodynamic parameters were examined for initial concentrations of 100 mg/L, pH 2 and absorbent dose of 1.5 g/L, including the changes in enthalpy (ΔH°), entropy (ΔS°) and free energy (ΔG°). The changes in enthalpy and entropy were estimated applying the following equations: [15,33].

$$\Delta G^\circ = -RT\ln K_C \tag{5}$$

$$\ln K_C = \frac{\Delta S^\circ}{R} - \frac{\Delta H^\circ}{RT} \tag{6}$$

where K_C (L/mol) is thermodynamic adsorption equilibrium constant and calculated by Eq. (7) below. Here, ΔS° (J/mol K) is standard entropy, ΔH° is standard enthalpy, T is the absolute temperature and R is the gas constant valued 8.314 J/(mol K). The values of ΔH° and ΔS° were determined from the slope and intercept of the fitted curve, respectively. The Gibbs free energy of adsorption (ΔG°) subsequently determined from the identified parameters ΔH° and ΔS° by Eq. (5). These values are given in Table 1.

$$K_C = \frac{q_e}{C_e} \tag{7}$$

where q_e is the equilibrium dye concentration on the adsorbent (mg/L) and C_e is the equilibrium dye concentration in solution (mg/L).

The positive values of ΔH° designate an endothermic adsorption process. The positive value of ΔS° propose an increase in RR2 at the solid solution interface during the adsorption process whereas the negative value of ΔG° demonstrations that the adsorption process is spontaneous in the studied temperature range. The increase in ΔG° with temperature indicates that more RR2 adsorbs at higher temperatures [34].

Table 1
Thermodynamic parameters for the adsorption of RR2 adsorption onto WAC

ΔH° (KJ/mol)	ΔS° (KJ/mol)	ΔG°(KJ/mol)		
		293	303	313
29.12	101.738	226.68	918.52	2106.43

3.7. Adsorption isotherms

The produced activated carbon was tested for its adsorption capacity. The amount of dye adsorbed can be determined as a function of the concentration at a constant temperature, which can be described by adsorption isotherms. In this study, analysis of the adsorption isotherms was carried out by applying the linear Langmuir equation [Eq. (8)], the Freundlich equation [Eq. (9)] [35] and Temkin equation [Eq. (10)] [36] as below:

$$\frac{C_e}{q_e} = \frac{1}{Q_m K_L} + \frac{C_e}{Q_m} \tag{8}$$

$$\ln(q_e) = \ln(K_f) + \frac{1}{n}\ln(C_e) \tag{9}$$

$$q_e = \frac{RT}{b}\ln(K_T) + \frac{RT}{b}\ln(C_e) \tag{10}$$

where C_e (mg/L) is the concentration of the dye at equilibrium; q_e (mg/g) is the amount of dye adsorbed per unit weight of activated carbon at equilibrium; K_L (L/mg) is a Langmuir constant related to the free energy of adsorption; and Q_m (mg/g) is the maximum adsorption capacity. K_F is a Freundlich constant indicating the relative adsorption capacity of the carbon, and $1/n$ is the adsorption intensity. RT/b = B (J/mol) and A (L/g) are Temkin constants, which are related to heat of sorption and maximum binding energy, respectively. R is the gas constant (8.31 J/mol K) and T (K) is the absolute temperature.

The Langmuir, Freundlich and Temkin plots for the process are presented in Fig. 9, and the isotherm constants and correlation coefficients are given in Table 2. The Langmuir, Freundlich and Temkin isotherms of WSAC were found to be linear over the whole concentration range, and the R^2 values showed that the Langmuir model fit better than the Freundlich and Temkin model. The maximum adsorption capacities according to Langmuir model for RR2 was determined as 81.3 mg/g (Table 2). Similar trends were shown for the adsorption of RR2 onto Hazelnut Shells [37] and Walnut shell [38].

3.9. Adsorption kinetics

Fitting the experimental data into different kinetic models enables to study the adsorption rate, model the process

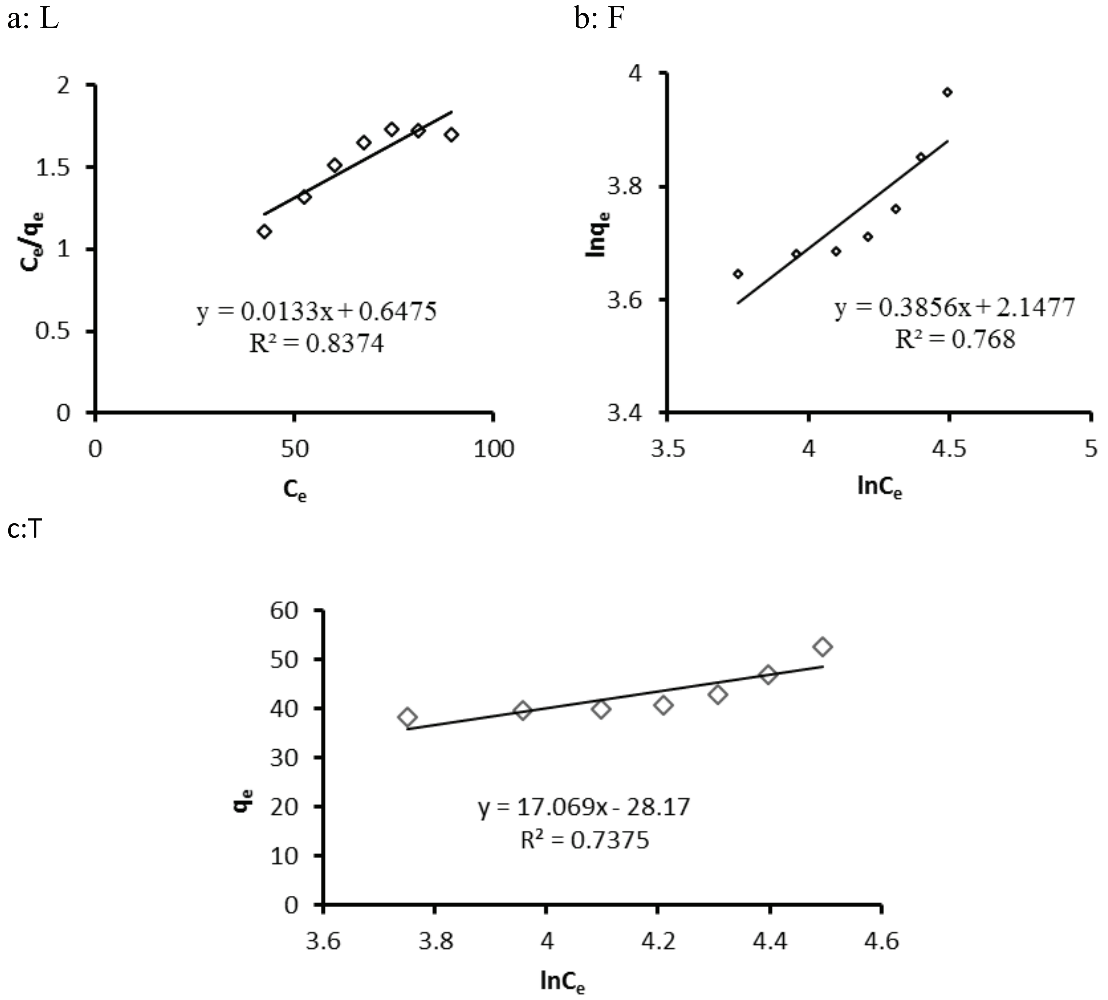

Fig. 9. Isotherm plots for the adsorption of RR2; a: Langmuir, b: Freundlich, and c:Temkin.

Table 2
Isotherm constants and correlation coefficients for the removal of RR2

Langmuir			Freundlich			Temkin		
q_m (mg/g)	b (L/mg)	R²	K_f (mg/g)(L/mg)$^{(1/n)}$	n	R²	β (J/mol)	K_T (L/g)	R²
81.3	0.017	0.834	7.39	2.35	0.822	17.069	1.65	0.737

and predict information about adsorbent/adsorbate interaction [39,40]. Several kinetic models have been applied to examine the controlling mechanism of dye adsorption from aqueous solution. In this study pseudo-first-order [19], pseudo-second–order [41], and intra-particle diffusion [41] and Elovich kinetic model [18] were applied.

Pseudo-First order model according to Eq. (11) has been used to investigate the rate constants for adsorption of dye onto WSAC [42].

$$\ln n\left(q_e - q_t\right) = \ln q_e - K_1 t \tag{11}$$

where k_1 is the Pseudo-first-order-rate constant, which can be attained from the slope of the plot $\ln(q_e - q_t)$ vs. time.

The coefficients of correlation for the Pseudo-first-order-kinetic model were not high for adsorbent at different concentrations and the estimated values of q_e calculated from the equation differed from the experimental values (Table 3), which demonstrates that the model is not suitable to describe the adsorption process. Therefore, the pseudo-second-order model has been developed to explain adsorption kinetics [Eq. (12)] [43]

$$\frac{t}{q_t} = \frac{1}{K_2 q_e^2} + \frac{1}{q_e} t \tag{12}$$

where k_2 is the second-order-rate constant (g/ mg·min). The values of k_2 at different initial dye concentrations was esti-

Table 3
Kinetic model constants and correlation coefficients for the removal of RR2

Dye Con. (mg/l)	Pseudo-first-order kinetic model		Pseudo-second-order kinetic model		Elovich model			Intraparticle diffusion equation	
	K_1 (min^{-1})	R^2	K_2 (g/ mg min)	R^2	β	α	R^2	K_p (mg/g min)	R^2
50	0.022	0.948	0.002	0.995	5.02	0.3	0.992	3.68	0.922
100	0.028	0.973	0.001	0.999	9.18	0.22	0.996	3.01	0.916
150	0.022	0.985	0.001	0.996	11.02	0.15	0.997	1.65	0.952

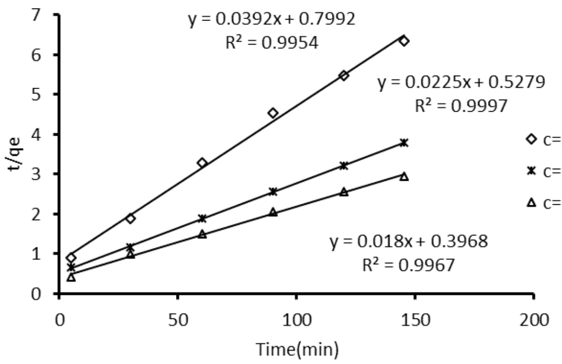

Fig. 10. Pseudo second-order kinetics at different RR2 concentration (adsorbent dose: 1 g and pH 2).

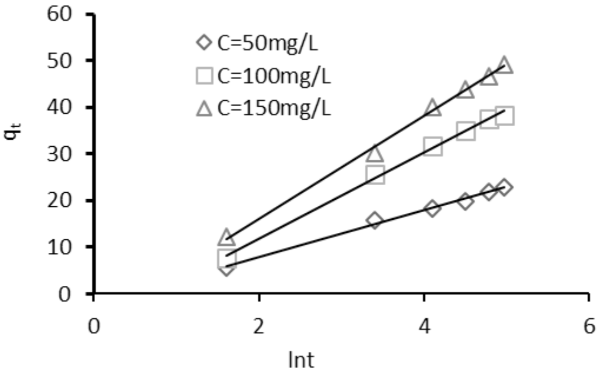

Fig. 11. Plots of Elovich for the sorption of RR2 on to WAC (adsorbent dose: 1 g and pH 2).

mated from the slopes of the respective linear plots of t/q_t vs. t.

The results in Fig. 10 show linear plots with very high values of R^2 (Table 3) in addition to the good agreement between experimental and calculated values of Eq. (12). Therefore, the adsorption of RR2 onto WSAC is greatly represented by the pseudo-second-order kinetic. Similar trends were shown for the adsorption of RR2 onto Metapenaeus monoceros shells hazelnut shells [44].

Fig. 11 shows a plot of the Elovich equation for the same data. In this case, a linear relationship was obtained between adsorbed RR2, q_t, and ln t over the whole adsorption period, with high correlation coefficients (> 0.992) for all the lines (Table 3). The same type of plot for the adsorption of RR2 on WSAC at various concentration of dye is shown in Fig. 11. The linear correlation coefficients were highly significant (> 0.992) and once more demonstrated a high degree of correlation between the experimental data and the theoretical data predicted by the Elovich model as defined by Eq. (13). It is clear that a simple Elovich equation may be used to describe the kinetics of adsorption of RR2 on WAC while an expression for a fractional power function kinetic reaction failed. Table 3 lists the kinetic constants obtained from the Elovich equation.

$$q_e = \frac{1}{\beta}\ln(\alpha\beta) + \frac{1}{\beta}\ln t \tag{13}$$

where α (mg/(g·min)) is the initial adsorption rate of the Elovich equation, and β (g/mg) is the desorption constant related to the extent of surface coverage and activation energy constant for chemisorption [15].

Thus, on increasing the initial RR2 concentration from 50 to 150 mg/L, the value of decreased from 0.3 to 0.15 mg/(g·min) and the value of β increased from 5 to 11 g/mg.

In order to investigate the mechanism of RR2 adsorption onto WSAC, intra-particle diffusion based mechanism was studied. It is proposed that the uptake of the adsorbate by the adsorbent varies almost proportionately with the square root of the contact time ($t^{1/2}$) according to Eq. (14) [39].

$$q_e = K_p t^{0.5} + C \tag{14}$$

where t (min) is the contact time, q_t (mg/g) is the dye uptake value at time t, k_p (mg /g min$^{1/2}$) is the intra-particle diffusion rate constant determined from the slopes of the linear plots, C is the constant, which indicates the thickness of the boundary layer. The larger value of C the greater effect on the boundary layer [45]. Thus, with increasing the initial RR2 concentration from 50 to 150 mg/L, the value of K_p (mg/g min) decreased from 3.68 to 1.65 mg/(g·min). The correlation coefficients was 0.95 that suggest a strong relationship between the parameters and explains that the process follows intra-particle diffusion model at the higher concentration of RR2 but not same as pseudo-second-order model (Table 3). The correlation coefficient was 0.99, which suggest a strong relationship between the parameters and explains that the process follows pseudo-second-order kinetics. The adsorption kinetic was studied at temperature 28°C; initial dye concentration (50, 100 and 150 mg/L); adsorbent dose: 1 g and

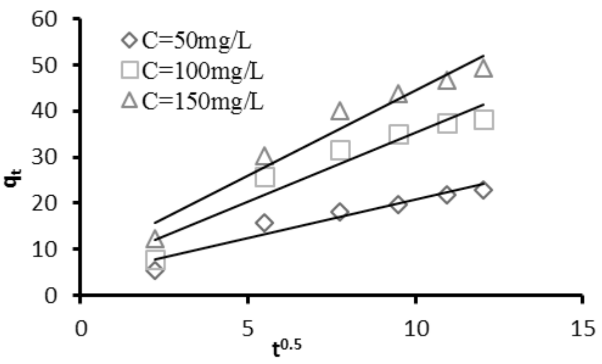

Fig. 12. Intra-particle diffusion equation kinetics at different RR2 concentration (adsorbent dose: 1 g and pH 2).

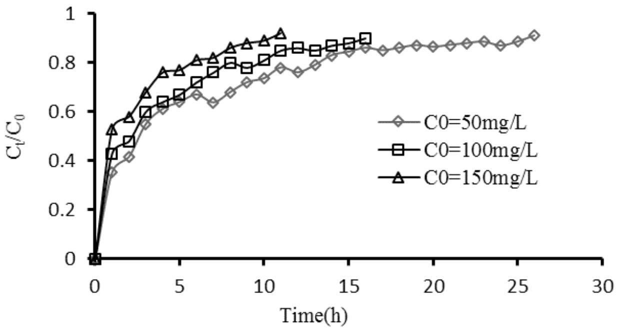

Fig. 13. Breakthrough curves for RR2 adsorption on prepared activated carbon at different initial dye concentrations (Q = 10 mL/min; bed height = 4cm).

pH2. Fig. 10 illustrates the kinetic models that are fitted to the experimental data. Similarly, all values of different kinetic parameters, as shown in Table 3 were obtained from various graphical presentations of kinetic equations. Data analyzing, mentioned that the highest R^2 value were found for the pseudo-order kinetic model.

3.10. Regeneration

Applied WSAC was regenerated by heat recovery and reused for adsorption. The absorption capacity of regenerated WSAC was 32.46 mg/g. However, the RR2 at high temperatures severance, but due to the closure of a number of the WSAC pores, absorption capacity decreased. One very important feature of absorbent for practical applications is ability of regeneration. The results showed that the WSAC as well as functionality is restored and reused. The results showed that there generation of granular activated carbon had good absorption capacity of 32.46 mg/g, which is about 85% of initial capacity.

3.11. Column studies

3.11.1. Effect of initial dye concentration

The effect of a variation of the inlet RR2 concentration from 50 to 150 mg/L have been investigated with the same adsorbent bed height of 4 cm, when other variable kept constant and solution flow rate was 10 mL/min. The breakthrough curve based on Thomas model has been drawn according to Fig. 13. The results showed that high concentration is cause of shorter time for media saturation and failure (breakthrough time). The bed adsorption capacity was increased with increasing concentration from 50 to 150 mg/L, that resulting increase in capacity from 42.18 to 53.72 mg/g. With increasing levels of input dye, the slope of breakthrough curve increased and breakthrough time occurred at less time in the bed. This mater suggests that changes in the concentration gradient has effect on breakthrough time and saturation time of the bed that can be explained by increasing the concentration of color, which can be cause of more absorption of dye molecules by the absorbent structure. Hence, it can be concluded that the adsorption process is dependent on the initial concentration of the substrate input. By increasing the initial concentration of dye (input loading of dye molecules) in the bed the (thrust to move more mass) driving force for mass transfer will increased and shorter the length of the mass transfer resulting the breakthrough in a short time [46,47].

The increasing of concentrations from 50 to 150 mg/L was cause of maximum adsorption per mass unit of adsorbent from 42.18 to 53.72 mg/g of the substrate. Studies by Chen et al. and Zambrano et al. showed same results at comparison with present research work [17,48].

3.11.2. Effect of bed height

Fig. 14 show graphical result of breakthrough curve at different height. The results show by increasing the bed height from 2 to 8 cm, the adsorption capacity increased from 37.28 to 54.61 mg/g (Table 4). According to Fig. 10, the slope of the breakthrough curved creased, when the bed height increased, which may result in more extensive of mass transfer area and increases the time to reach the saturation point in column. As mentioned by researchers increasing absorption capacity can be due to adsorption time increasing [32] and increase in the surface area of adsorbent, which provide more binding sites for adsorption [49].

3.11.3. Effect of flow rate

Fig. 15 shows results of breakthrough curve at different flow conditions. The results showed by increasing the flow rate, time to break point and saturation was decreased. Also with increasing flow rate from 5 to 15 mL/min, the bed capacity adsorption was reduced from 51.81 to 36.67 mg/g (Table 4). This result showed that adsorption process is dependent on flow rate and with increasing of flow, the breakthrough curves became steeper and the breakthrough time will happen at shorter period. The reason for this has been mentioned at previous research works that when the input flow rate increase, the imbalance situation between adsorbent and adsorbate because of not sufficient contact time will occur, which is result of constant stations in the fixed bed [47]. Therefore, when the residence time of the solute in the column is not long enough for adsorption equilibrium to be reached at that flow rate, the RR2 solu-

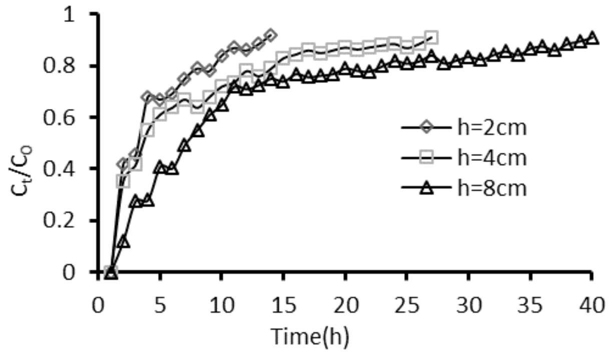

Fig. 14. Breakthrough curves for RR2 adsorption on prepared activated carbon at different bed heights (Q = 10 mL/min; C_0= 50 mg/L).

Table 4
The operation parameters of column and Thomas model

h (cm)	Q (mL/min)	C_0 (mg/L)	K_{th} (mL mg^{-1}min^{-1})	q_0 (mg/g)
2	10	50	0.0112	37.28
4	10	50	0.015	42.18
8	10	50	0.0172	54.61
4	5	50	0.01	51.81
4	15	50	0.017	36.67
4	10	100	0.0064	49.36
4	10	150	0.0052	53.72

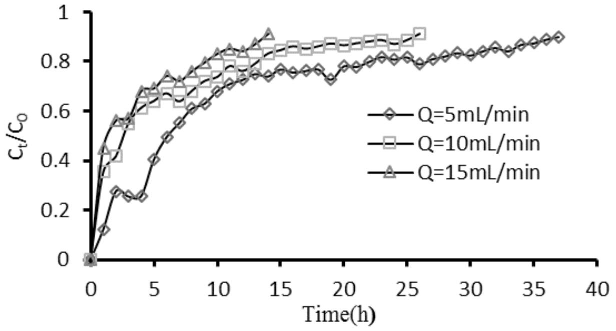

Fig. 15. Breakthrough curves for RR2 adsorption on prepared activated carbon at different flow rate (h = 4 cm; C_0= 50 mg/L).

tion leaves the column before equilibrium occurs [50]. The results of investigation by different researchers confirm result of present work [51] and [52].

4. Conclusions

In this study, the adsorption of Reactive Red 2 onto walnut shell activated carbon in batch and fixed-bed systems has been investigated. The effect of the initial dye concentration and operating parameters on the breakthrough curves and column adsorption parameters was examined.

The outcomes show that all the parameters have a significant effect on the adsorption of RR2 onto walnut shell.

The BET and SEM tests showed that WSAC has suitable surface area with pore volume of 0.453 cm^3/g. The FTIR spectrum of WSAC, indicates the presence of various functional groups at different wavelengths.

The aforementioned isotherm models confirmed that the equilibrium data are well represented by Langmuir model for RR2, which is valid for monolayer adsorption onto a surface containing a finite number of identical sites. Kinetics study shows the adsorption reaction follows pseudo-second order kinetic model (R^2 = 0.999).

The positive values of $\Delta H°$ indicate an endothermic adsorption process. The positive value of $\Delta S°$ suggests an increase in RR2 at the solid solution interface during the adsorption process.

Tomas model was applied to experimental data obtained from column studies to predict the breakthrough curves and to determine the kinetic parameters. The initial region of the breakthrough curve is well described by the model for all studied conditions. The strong effect of the variables suggests that the adsorption of dye onto walnut shell is influenced by mass transfer limitations, probably due to the weak intra-particle diffusion of the dye into the walnut shell pores. The results consistently showed that the increase in input color and height of the adsorption capacity of column increased. The results showed that by increasing of flow rate the adsorption capacity was reduced.

Due to high absorption capacity of activated carbon of walnut shell, this material can serve as a good absorbent, indigenous and available as an alternative to the standard carbon, for treating water and wastewater.

Acknowledgements

The authors would like to thank Kermanshah University of medical science (KUMS) for financial support of this research project that has been performed by student with ID: 92170, through Grant No. 92026 and the Department of environmental health Engineering, KUMS for the use of facilities.

References

[1] S. Dawood, T.K. Sen, C. Phan, Synthesis and characterisation of novel-activated carbon from waste biomass pine cone and its application in the removal of congo red dye from aqueous solution by adsorption, Water Air Soil Pollut., 225 (2014) 1–16.

[2] R. Han, Y. Wang, X. Zhao, Y. Wang, F. Xie, J. Cheng, M. Tang, Adsorption of methylene blue by phoenix tree leaf powder in a fixed-bed column: experiments and prediction of breakthrough curves, Desalination, 245 (2009) 284–297.

[3] Y. Feng, F. Yang, Y. Wang, L. Ma, Y. Wu, P.G. Kerr, L. Yang, Basic dye adsorption onto an agro-based waste material–Sesame hull (Sesamum indicum L.), Bioresour. Technol., 102 (2011) 10280–10285.

[4] E.C. Lima, B. Royer, J.C. Vaghetti, N.M. Simon, B.M. da Cunha, F.A. Pavan, E.V. Benvenutti, R. Cataluña-Veses, C. Airoldi, Application of Brazilian pine-fruit shell as a biosorbent to removal of reactive red 194 textile dye from aqueous solution: kinetics and equilibrium study, J. Hazard. Mater., 155 (2008) 536–550.

[5] F. Banat, S. Al-Asheh, R. Al-Ahmad, F. Bni-Khalid, Bench-scale and packed bed sorption of methylene blue using treated olive pomace and charcoal, Bioresour. Technol., 98 (2007) 3017–3025.

[6] Z.Z. Chowdhury, S.B.A. Hamid, R. Das, M.R. Hasan, S.M. Zain, K. Khalid, M.N. Uddin, Preparation of carbonaceous adsorbents from lignocellulosic biomass and their use in removal of contaminants from aqueous solution, BioResources., 8 (2013) 6523–6555.

[7] H. Wang, X.-W. Zheng, J.-Q. Su, Y. Tian, X.-J. Xiong, T.-L. Zheng, Biological decolorization of the reactive dyes Reactive Black 5 by a novel isolated bacterial strainEnterobactersp. EC3, J. Hazard. Mater., 171 (2009) 654–659.

[8] M. Costa, S. Mota, R. Nascimento, A. Dos Santos, Anthraquinone-2, 6-disulfonate (AQDS) as a catalyst to enhance the reductive decolourisation of the azo dyes Reactive Red 2 and Congo Red under anaerobic conditions, Bioresour. Technol., 101 (2010) 105–110.

[9] F. Moghadasi, M. Momen Heravi, M. Bozorgmehr, P. Ardalan, T. Ardalan, Kinetic and thermodynamic study on the removal of methyl orange from aqueous solution by adsorption onto Camel Thorn Plant, Asian J. Chem., 22 (2010) 5093–5100.

[10] M. Kermani, H. Pourmoghaddas, B. Bina, Z. Khazaei, Removal of phenol from aqueous solutions by rice husk ash and activated carbon, PJBS., (2006) 1905–1910.

[11] J. Yang, K. Qiu, Preparation of activated carbons from walnut shells via vacuum chemical activation and their application for methylene blue removal, Chem. Eng. J., 165 (2010) 209–217.

[12] Z.Z. Chowdhury, S.M. Zain, R.A. Khan, A. Arami-Niya, K. Khalid, Process variables optimization for preparation and characterization of novel adsorbent from lignocellulosic waste, BioResources., 7 (2012) 3732–3754.

[13] Ministry of agriculture. Department of planning and economy statistical office of information technology publication., (2002/03) 72–74.

[14] X.S. Wang, Z.Z. Li, S.R. Tao, Removal of chromium (VI) from aqueous solution using walnut hull, J. Environ. Manage., 90 (2009) 721–729.

[15] J.-S. Cao, J.-X. Lin, F. Fang, M.-T. Zhang, Z.-R. Hu, A new absorbent by modifying walnut shell for the removal of anionic dye: Kinetic and thermodynamic studies, Bioresour. Technol., 163 (2014) 199–205.

[16] X. Song, Y. Pan, Q. Wu, Z. Cheng, W. Ma, Phosphate removal from aqueous solutions by adsorption using ferric sludge, Desalination, 280 (2011) 384–390.

[17] J. Barron-Zambrano, A. Szygula, M. Ruiz, A.M. Sastre, E. Guibal, Biosorption of Reactive Black 5 from aqueous solutions by chitosan: Column studies, J. Environ. Manage., 91 (2010) 2669–2675.

[18] S. Kaur, S. Rani, R.K. Mahajan, Adsorption kinetics for the removal of hazardous dye congo red by biowaste materials as adsorbents, J. Chem., 2013 (2012) 1–12.

[19] A.M. Aljeboree, A.N. Alshirifi, A.F. Alkaim, Kinetics and equilibrium study for the adsorption of textile dyes on coconut shell activated carbon, Arabian J. Chem., (2014).

[20] M.K. Dahri, M.R.R. Kooh, L.B. Lim, Water remediation using low cost adsorbent walnut shell for removal of malachite green: equilibrium, kinetics, thermodynamic and regeneration studies, JECE., 2 (2014) 1434–1444.

[21] L. Zhang, H. Xia, J. Peng, S. Zhang, S. Wang, Preparation of high specific surface area activated carbon from walnut shells by microwave-induced KOH activation, J. Porous Mater., 22 (2015) 1527–1537.

[22] J. Song, W. Zou, Y. Bian, F. Su, R. Han, Adsorption characteristics of methylene blue by peanut husk in batch and column modes, Desalination, 265 (2011) 119–125.

[23] N. Azouaou, Z. Sadaoui, H. Mokaddem, Adsorption of Lead from Aqueous Solution onto Untreated Orange Barks: Equilibrium, Kinetics and Thermodynamics, E3S Web of Conferences, EDP Sciences., 2013, pp. 41034.

[24] K. Kadirvelu, C. Faur-Brasquet, P.L. Cloirec, Removal of Cu (II), Pb (II), and Ni (II) by adsorption onto activated carbon cloths, Langmuir., 16 (2000) 8404–8409.

[25] T. Anirudhan, M. Ramachandran, Adsorptive removal of basic dyes from aqueous solutions by surfactant modified bentonite clay (organoclay): Kinetic and competitive adsorption isotherm, Process Saf. Environ. Prot., 95 (2015) 215–225.

[26] K. Chinoune, K. Bentaleb, Z. Bouberka, A. Nadim, U. Maschke, Adsorption of reactive dyes from aqueous solution by dirty bentonite, Appl. Clay Sci., 123 (2016) 64–75.

[27] R. Elmoubarki, F. Mahjoubi, H. Tounsadi, J. Moustadraf, M. Abdennouri, A. Zouhri, A. El Albani, N. Barka, Adsorption of textile dyes on raw and decanted Moroccan clays: Kinetics, equilibrium and thermodynamics, Water Resour. Indus., 9 (2015) 16–29.

[28] A.A. Nunes, A.S. Franca, L.S. Oliveira, Activated carbons from waste biomass: an alternative use for biodiesel production solid residues, Bioresour. Technol., 100 (2009) 1786–1792.

[29] X.-q. Zeng, Sorption of wastewater containing reactive red X-3B on inorgano-organo pillared bentonite, J Zhejiang Univ Sci B., 7 (2006) 314–319.

[30] M. Manoochehri, V. Rattan, A. Khorsand, H.A. Panahi, Capacity of activated carbon derived from agricultural waste in the removal of reactive dyes from aqueous solutions, Carbon Lett.., 11 (2010) 169–175.

[31] B. Hameed, D. Mahmoud, A. Ahmad, Equilibrium modeling and kinetic studies on the adsorption of basic dye by a low-cost adsorbent: Coconut (Cocos nucifera) bunch waste, J. Hazard. Mater., 158 (2008) 65–72.

[32] M. Auta, B. Hameed, Chitosan–clay composite as highly effective and low-cost adsorbent for batch and fixed-bed adsorption of methylene blue, Chem. Eng. J., 237 (2014) 352–361.

[33] R.I. Yousef, B. El-Eswed, H. Ala'a, Adsorption characteristics of natural zeolites as solid adsorbents for phenol removal from aqueous solutions: kinetics, mechanism, and thermodynamics studies, Chem. Eng. J., 171 (2011) 1143–1149.

[34] J. Shah, M.R. Jan, A. Haq, Y. Khan, Removal of Rhodamine B from aqueous solutions and wastewater by walnut shells: kinetics, equilibrium and thermodynamics studies, Fresenius. Chem. Sci Eng., 7 (2013) 428–436.

[35] A.N. Moghaddam, G. Najafpour, A. Ghoreyshi, M. Mohammadi, Adsorption of methylene blue in aqueous phase by fly ash, clay and walnut shell as adsorbents, World Appl Sci J., 8 (2010) 229–234.

[36] Z.N. Garba, A.A. Rahim, Evaluation of optimal activated carbon from an agricultural waste for the removal of para-chlorophenol and 2, 4-dichlorophenol, Process Saf. Environ. Prot., 102 (2016) 54–63.

[37] A. Al-Sharify, Z. Athab, A. Halbus, Adsorption of Reactive Red 2 Dye onto activated Carbon prepared from Hazelnut Shells, Iraqi, Nat. Journ. Chem., 51 (2013) 273–387.

[38] A. Almasi, S.A. Mousavi, A. Hesari, H. Janjani, Walnut shell as a natural adsorbent for the removal of Reactive Red 2 form aqueous solution, IRJABS., 10 (2016) 551–556.

[39] T.M. Elmorsi, Z.H. Mohamed, W. Shopak, A.M. Ismaiel, Kinetic and equilibrium isotherms studies of adsorption of Pb (II) from water onto natural adsorbent, J. Environ. Prot., 5 (2014) 1667.

[40] A.E. Martins, M.S. Pereira, A.O. Jorgetto, M.A. Martines, R.I. Silva, M.J. Saeki, G.R. Castro, The reactive surface of Castor leaf [Ricinus communis L.] powder as a green adsorbent for the removal of heavy metals from natural river water, Appl. Surf. Sci., 276 (2013) 24–30.

[41] G. Vijayakumar, R. Tamilarasan, M. Dharmendirakumar, Adsorption, kinetic, equilibrium and thermodynamic studies on the removal of basic dye Rhodamine-B from aqueous solution by the use of natural adsorbent perlite, J. Mater. Environ. Sci., 3 (2012) 157–170.

[42] M. Matouq, N. Jildeh, M. Qtaishat, M. Hindiyeh, M.Q. Al Syouf, The adsorption kinetics and modeling for heavy metals removal from wastewater by Moringa pods, JECE., 3 (2015) 775–784.

[43] B. Makhoukhi, M. Djab, M.A. Didi, Adsorption of Telon dyes onto bis-imidazolium modified bentonite in aqueous solutions, JECE., 3 (2015) 1384–1392.

[44] E. Thiyagarajan, P. Saravanan, S. Shiyamala devi, P. Saranya, N. Nagendra Gandhi, S. Renganathan, Biosorption of reactive red 2 using positively charged Metapenaeus monoceros shells, J. Saudi Chem. Soc., 21 (2017) S1–S6.

[45] D. Ding, Y. Zhao, S. Yang, W. Shi, Z. Zhang, Z. Lei, Y. Yang, Adsorption of cesium from aqueous solution using agricultural residue–Walnut shell: Equilibrium, kinetic and thermodynamic modeling studies, Water Res., 47 (2013) 2563–2571.

[46] A. Ahmad, B. Hameed, Fixed-bed adsorption of reactive azo dye onto granular activated carbon prepared from waste, J. Hazard. Mater., 175 (2010) 298–303.

[47] Z.Z. Chowdhury, S.M. Zain, R.A. Khan, R.F. Rafique, K. Khalid, Batch and fixed bed adsorption studies of lead (II) cations from aqueous solutions onto granular activated carbon derived from Mangostana garcinia shell, BioResources., 7 (2012) 2895–2915.

[48] S. Chen, Q. Yue, B. Gao, Q. Li, X. Xu, K. Fu, Adsorption of hexavalent chromium from aqueous solution by modified corn stalk: A fixed-bed column study, Bioresour. Technol., 113 (2012) 114–120.

[49] W. Li, Q. Yue, P. Tu, Z. Ma, B. Gao, J. Li, X. Xu, Adsorption characteristics of dyes in columns of activated carbon prepared from paper mill sewage sludge, Chem. Eng. J., 178 (2011) 197–203.

[50] X. Xu, B. Gao, X. Tan, X. Zhang, Q. Yue, Y. Wang, Q. Li, Nitrate adsorption by stratified wheat straw resin in lab-scale columns, Chem. Eng. J., 226 (2013) 1–6.

[51] A. Goshadrou, A. Moheb, Continuous fixed bed adsorption of CI Acid Blue 92 by exfoliated graphite: An experimental and modeling study, Desalination, 269 (2011) 170–176.

[52] L. Cavas, Z. Karabay, H. Alyuruk, H. Doğan, G.K. Demir, Thomas and artificial neural network models for the fixed-bed adsorption of methylene blue by a beach waste Posidonia oceanica (L.) dead leaves, Chem. Eng. J., 171 (2011) 557–562.